

# Lattice Boltzmann implementation for Fluids Flow Simulation in Porous Media

Xinming Zhang

*Department of Mathematics and Natural Science  
Harbin Institute of Technology Shenzhen Graduate School  
Shen zhen China  
xinmingxueshu@gmail.com*

**Abstract**-In this paper, the lattice-Boltzmann method is developed to investigate the behavior of isothermal two-phase fluid flow in porous media. The method is based on the Shan-Chen multiphase model of nonideal fluids that allow coexistence of two phases of a single substance. We reproduce some different idealized situations (phase separation, surface tension, contact angle, pipe flow, and fluid droplet motion, et al) in which the results are already known from theory or laboratory measurements and show the validity of the implementation for the physical two-phase flow in porous media. Application of the method to fluid intrusion in porous media is discussed and shows the effect of wettability on the fluid flow. The capability of reproducing critical flooding phenomena under strong wettability conditions is also proved.

**Index Terms** - Multiphase Fluids, Porous Media, Simulation, Lattice Boltzmann Method

## I. INTRODUCTION

Two-phase flows are encountered in many natural and industrial processes, including soil pollution and remediation, enhanced oil recovery, emulsion flow and stability, etc, and have considerable economic and scientific importance in these practical problems and applications. However, due to the inherent complexity of two-phase flows, from a physical as well a numerical point of view, “general” applicable computational fluid dynamics (CFD) codes are non-existent.

In the last few years the lattice Boltzmann method (LBM) which is based on the cellular automaton concept, has attracted much attention as a CFD approach in fluids engineering [1, 2]. The LBM is based on statistical (macroscopic) description of microscopic phenomena. It describes a fluid as an ensemble of many particles interacting locally at the nodes of a regular lattice by collisions. And it has been shown to recover the conservation laws of continuum fluid dynamics, and, thus, allows the calculation of the macroscopic variables such as density and velocity. For its unique derivation, LBM has some advantages over the conventional computational methods. All information transfer is local in time and space and, thus, the algorithms can easily be implemented on parallel computers. It’s locality with respect to computational mesh is absolutely essential for

the applications of interfacial problems. In addition, it has particular significance for porous media because LBM can easily simulate fluid flow with highly complex solid or free boundaries relative to continuum modeling approaches.

To date, a number of different approaches have been used to simulate the two-phase fluid flows, including Chromodynamic model [3], Shan-Chen model[4], free-energy model[5] and HSD model[6], etc. All these models have their own advantages in the simulation of two-phase flow. The purpose of the research presented in this paper is to investigate the behavior of isothermal two-phase fluid flow in porous media using the single component, two-phase lattice-Boltzmann model, developed by Shan and Chen. Although this model has some shortcoming, it is exceptionally versatile, and problems that have long defied quantitative treatment can now be examined. Here, we develop a two-phase flow simulator and demonstrate the applicability of the LBM for prescribing fluid properties for non-ideal fluids. We also present flow simulation results in the interior of porous media.

## II. LATTICE BOLTZMANN METHOD

Unlike traditional numerical methods which solve for the macroscopic variables, such as velocity and density, the LBM is based on the microscopic kinetic equation for the particle distribution function. The macroscopic quantities are obtained through moment integration of the distribution function. There are several different lattice-Boltzmann models available. In this paper we use the so-called lattice-BGK model [7], which is the simplest one in the hierarchy of lattice-Boltzmann methods.

The physical space is divided into a regular lattice and the velocity space is discretized into a finite set of velocities  $\{c_\alpha\}$ , the Boltzmann equation with BGK approximation can be discretized as

$$f_\alpha(\mathbf{x}_i + \mathbf{c}_\alpha \Delta t, t + \Delta t) - f_\alpha(\mathbf{x}_i, t) = -\frac{f_\alpha(\mathbf{x}_i, t) - f_\alpha^{eq}(\mathbf{x}_i, t)}{\tau} \quad (1)$$

Where  $\Delta t$  and  $\mathbf{c}_\alpha \Delta t$  are time and space increments, respectively.  $f_\alpha$  is the single-particle velocity distribution function along the  $\alpha$ th direction.  $f_\alpha^{eq}$  is the equilibrium distribution function, and  $\tau$  is the single relaxation time. In the simulations presented in this paper, we consider the two-dimensional square lattice with nine velocities-D2Q9 model. In this model the equilibrium distribution function is

$$f_\alpha^{eq} = \rho w_\alpha \left[ 1 + \frac{3}{c^2} \mathbf{c}_\alpha \cdot \mathbf{u} + \frac{9}{2c^4} (\mathbf{c}_\alpha \cdot \mathbf{u})^2 - \frac{3}{2c^2} \mathbf{u} \cdot \mathbf{u} \right] \quad (2)$$

where  $w_0 = 4/9$ ,  $w_1 = w_2 = w_3 = w_4 = 1/9$ , and  $w_5 = w_6 = w_7 = w_8 = 1/36$ . The macroscopic density  $\rho$  and velocity  $\mathbf{u}$  are related to the distribution function by

$$\rho = \sum_{\alpha=1}^9 f_\alpha \quad \text{and} \quad \rho \mathbf{u} = \sum_{\alpha=1}^9 f_\alpha \mathbf{c}_\alpha \quad (3)$$

To model surface tension forces that are characterized by a non-ideal gas equation of state, a nearest and next-nearest neighbor interaction potential can be incorporated into the lattice-Boltzmann model. We have adopted the method developed by Shan and Chen, where in addition to the local collisions neighboring fluid particles exchange momentum through an attractive short-range force:

$$\mathbf{F}(\mathbf{x}, t) = -G \psi(\rho(\mathbf{x}, t)) \sum_{\alpha=1}^8 w_\alpha \psi(\rho(\mathbf{x} + \mathbf{c}_\alpha \Delta t, t)) \mathbf{c}_\alpha \quad (4)$$

Where  $G$  is the interaction strength,  $w_\alpha$  is weight coefficient, and  $\psi(\rho(x, t))$  is the interaction potential:  $\psi(\rho) = \psi_0 e^{-\rho_0/\rho}$ ,  $\psi_0$ ,  $\rho_0$  are arbitrary constants.

Adhesive forces between the fluid and solid phases are introduced into the model by Martys[8]:

$$\mathbf{F}_{ads} = -G_{ads} \psi(\mathbf{x}, t) \sum_{\alpha} w_\alpha s(\mathbf{x} + \mathbf{c}_\alpha \Delta t) \mathbf{c}_\alpha \quad (5)$$

Here  $s = 0, 1$  for nodes in the liquid and on solid walls, respectively.  $G_{ads}$  represents the particle interaction strength between fluid and solid walls, and varying the  $G_{ads}$  parameter allows simulation of the complete range of contact angles.

With these definitions, in simulation, the cohesive force and the attractive force are added to the velocities that compute the equilibrium distribution function with the following formula:

$$\mathbf{u}^{eq} = \mathbf{u} + \Delta \mathbf{u} = \mathbf{u} + \mathbf{F}_{cohesive} / \omega \rho + \mathbf{F}_{adhesive} / \omega \rho \quad (6)$$

Where  $\omega = 1/\tau$  is the relaxation time,  $\rho$  is the density.

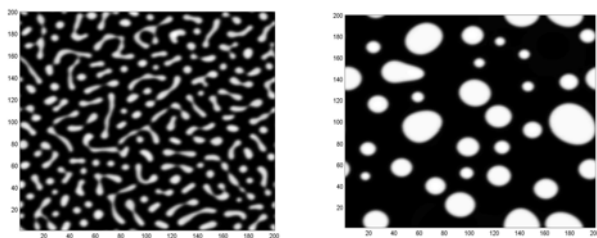
### III. RESULTS AND DISCUSSION

The ultimate success of the LBM for simulating liquid-vapor phenomena in porous media depends on its

ability to reproduce observed behavior, which for simple geometries is well described by physicochemical models. In this section, we demonstrate the applicability of the aforementioned algorithms for prescribing fluid properties in the context of the lattice-Boltzmann model for nonideal fluids, including phase separation, surface tension, contact angle, pipe flow, and fluid droplet motion.

In the case of multiphase flow, special care should be taken to ensure stable phase separation. Firstly, we present the results of numerical simulations for a two-dimensional system in which a first-order phase transition occurs. The numerical simulations reported here are on a 2D  $200 \times 200$  square lattices; and we took  $\psi_0 = 6.0$ ,  $\rho_0 = 100$  and  $\rho_c = \langle \rho \rangle = \rho_0 = 100$ . In the LBM simulation, the initial density distribution is homogeneous and a small (1%) random density noise is assigned to all grid points. Snapshots of the phase separation process at a series of times are shown in Fig.1. It can be seen from Fig.1 that, a part of original single-phase fluid rapidly condensed, and the average size of each of the coexisting phase domains tends to increase in an effort to decrease the interfacial energy. This corresponds, on a mesoscopic scale, to the randomization of the macroscopic velocity field as the system separates, as shown Fig.1. Liquid drops are formed depend on the total mass in the domain and consequently on the initial density selected, different initial condition resulted in different results. In Fig.1, several liquid drops are formed in a vapor atmosphere with initial density distribution  $\rho = (1.5 - (0.5 - rand) / 100) \rho_c$  and  $G_d = -28$ . The 'rand' is a random number in the interval  $[0, 1]$  generated by Fortran.

The second test is to estimate the surface tension. A series of simulations for a static two-dimensional liquid droplet are conducted and the pressure difference across the liquid-vapor interface and the droplet radius are used to compute the surface tension. For a two-dimensional droplet, the Laplace equation shows that the pressure difference,  $\Delta P = P_{in} - P_{out}$  across the surface of a static 2D droplet is related to the surface tension  $\sigma$  by  $\Delta P = \frac{\sigma}{r}$ , where  $P_{in}$  and  $P_{out}$  are the interior and exterior pressure, respectively, and  $r$  is the droplet radius.



T=100

T=1000

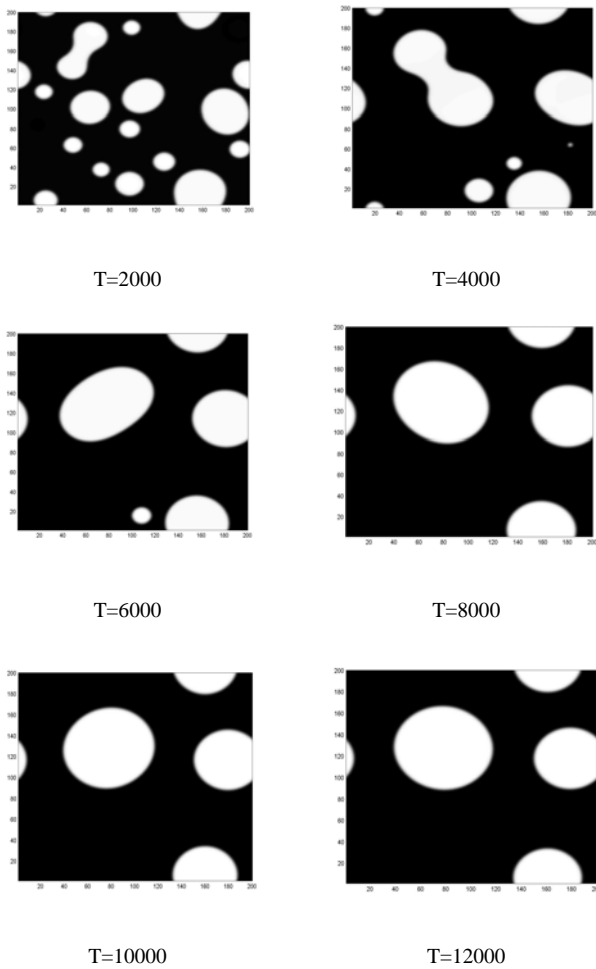


Fig.1 Time series of liquid-vapor phase separation dynamic

The initial condition is a droplet suspended in a vapor. The droplet is determined to be in equilibrium when the shape changes are insignificant. Fig.2 demonstrates the density profiles of the droplet when equilibrium state reaches, and Fig.3 shows the density and pressure profiles along the center line of the droplet. The size of the system in two dimensions is  $200 \times 200$  computational grid. The center of the droplet is located at the center of the computational grid. The initial density of liquid and vapor are  $\rho_{gas} = 50$ ,  $\rho_{liquid} = 250$ . It is obvious that there is a pressure difference inside and outside the droplet. The pressure inside the droplet is constant up to the interface (note that, the interface has a small but finite thickness), and is constant outside the droplet. A rapid pressure change occurs across the droplet interface. The difference between the two constant values is then use to compute the surface tension.

A number of tests with droplet radii ranging from 15 to 50 were run. The results are shown in Fig.4. The plot shows that a linear relationship between the pressure difference and the mean curvature is consistent with the assumption that the assumed equations of state would lead to a fluid with properties compatible with those used in standard CFD simulations. The pressure-radius relation fits the linear equation given below:

$$\Delta P = 3.5602 \frac{1}{r} + 0.0009$$

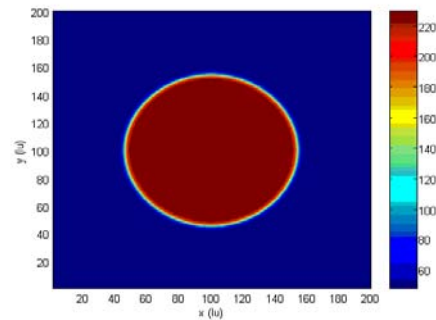


Fig.2 Equilibrium density profile(  $r = 50$  )

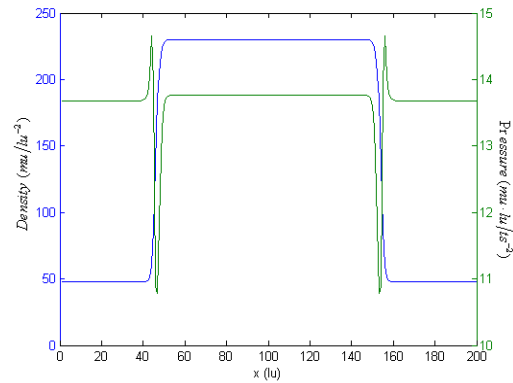


Fig.3 Density and pressure profiles along the center line of the droplet (  $r = 50$  )

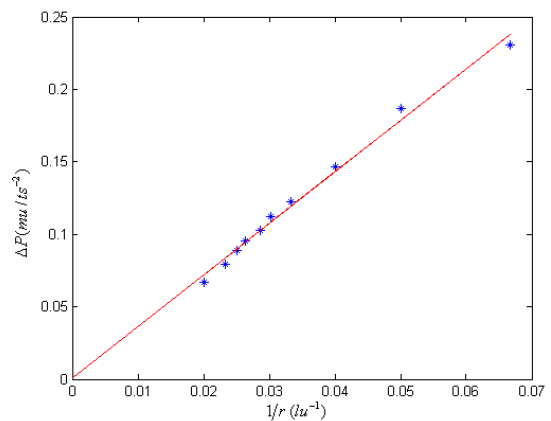


Fig.4  $\Delta P$  vs.  $1/r$  obtained through simulation

The relation between contact angle and the adhesive force constant  $G_{ads}$  is studied next. Fig.5 shows the different contact angles for different adhesive force constant. As the  $G_{ads}$  decreases, we can observe that the contact angle decreases because of the adhesive force between the fluid-solid grows stronger. The fluid region

is initially composed of a partial liquid droplet of radius 40 lu on the bottom solid wall of a  $200 \times 200$  lu box where the solid surface is at 0 through 2 lu in the y direction and the vapor phase elsewhere. In the simulations the non-slip boundary condition at solid-fluid interfaces is realized through a computationally efficient ‘bounce-back’ condition, where the particle momenta are conserved during collisions with a solid wall.

The relation between contact angle and the parameter  $G_{ads}$  is shown as Fig.6, and fits the linear equation given below:

$$\theta = 2.2025G_{ads} + 221.2598$$

Moreover, through the simulations, we found that high value of  $G_{ads}$  ( $G_s = -100$ ) leads to compression of the liquid near surfaces causing anomalously high liquid densities. All of these simulations are together with  $G = -25$  for the liquid cohesion and the particular EOS parameters.

The drainage process and imbibition process in a pipe are simulated in the Fig.7 and Fig.8. In the simulations, the no-slip boundary condition at solid-fluid interfaces is realized through a computationally efficient ‘bounce-back’ condition, and periodic condition was applied in the x-direction. Fig.7 and Fig.8 show simple pipe models with four different diameters ( $r = 10, 7, 5, 2$ , respectively). We used the same values of pressure gradient ( $F = 0.001$ ), cohesive force and adhesive force ( $G = -30, G_{ads} = -110$ ) for all models. Fig.7 shows drainage in which the non-wetting fluid is pumped into the wetting-fluid-saturated system and Fig.8 shows imbibition where the wetting fluid replaces the non-wetting fluid. As the diameter of the pipe increases, we can observe that the contact angles decrease accordingly because the capillary pressure decreases. It is also observed that the contact angle at imbibition ( $\theta_2$ ) is greater than that at drainage ( $\theta_1$ ). This is the well known contact angle hysteresis [9]. The simulation successfully shows the capillary hysteresis.

Fig. 9 presents simulated snapshots of the motion of a deformable liquid droplet in a straight channel with two solid barriers. The lattice is initially populated with the lighter phase –vapor, and a fluid layer is placed close to the upper channel end. Non-slip boundary conditions are imposed on the channel walls and on the barriers. Periodic boundary conditions are imposed on the two channel ends. In the first stage of the simulation, the liquid layer is given sufficient time -about 1500 time steps to relax and adopt a circular shape; then, force-driven flow is imposed to the modified velocity for equilibrium distribution function with  $adforce = 0.1 \times 10^{-4}$  acting in the negative y direction. It is interesting to note that the liquid droplet follows a pathway that drives it through the right opening, which is wider than the left two openings and, consequently, presents a slightly smaller capillary resistance.

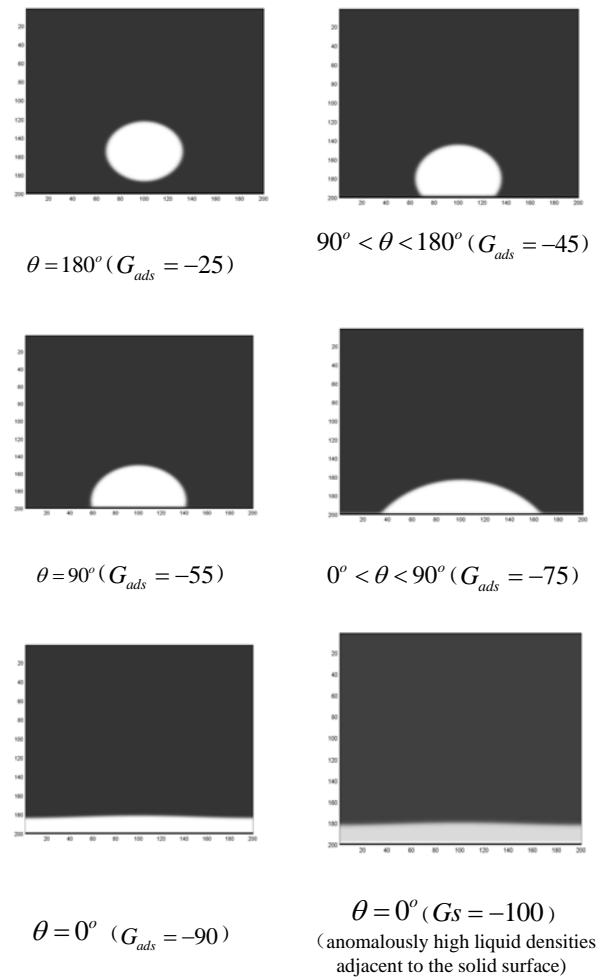


Fig.5 Different contact angles for different adhesive force constant

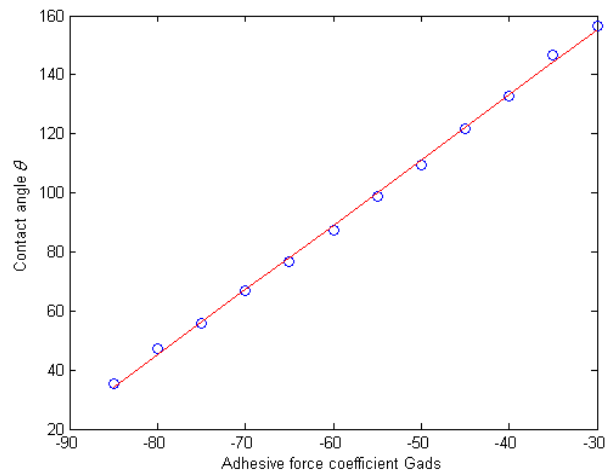


Fig.6 Contact angle vs. adhesive force coefficient

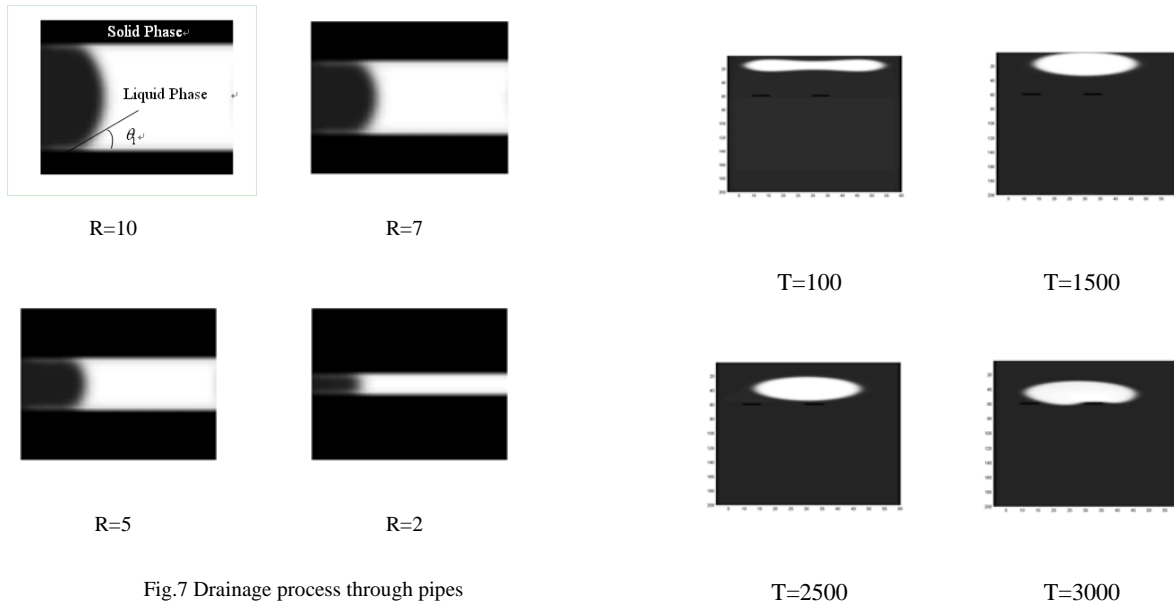


Fig.7 Drainage process through pipes

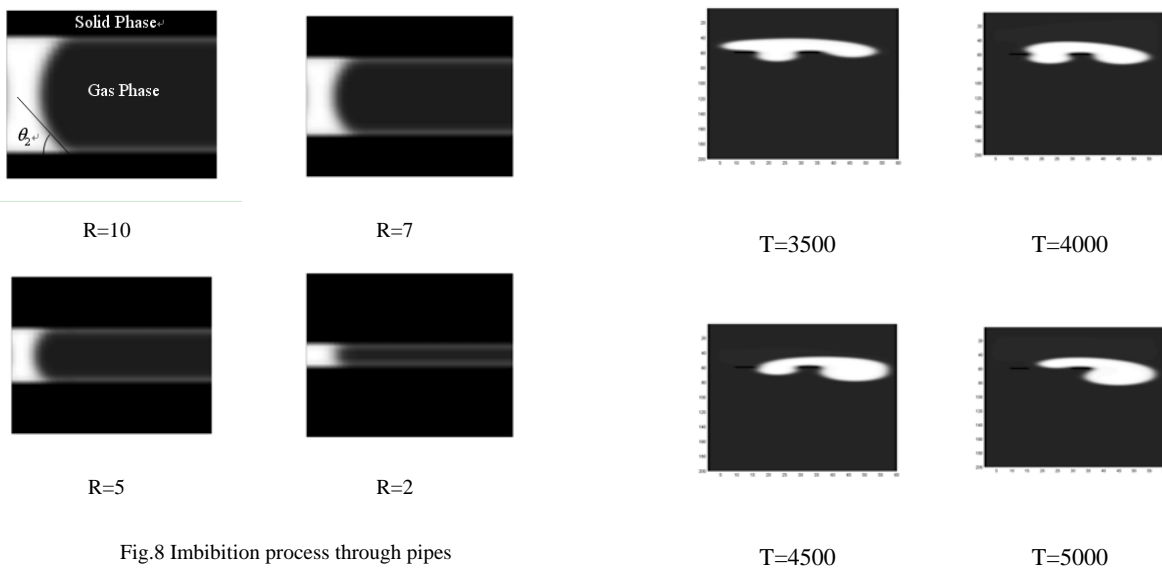
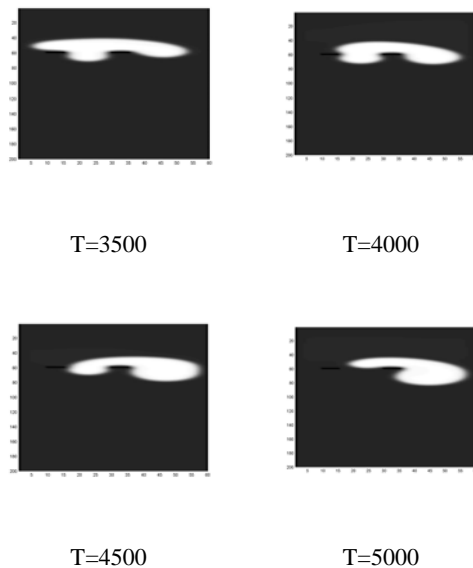


Fig.8 Imbibition process through pipes

Fig. 9 Motion of a deformable 2D liquid droplet in a channel with two solid obstacles



#### IV VAPOR-LIQUID TWO-PHASE FLOW SIMULATION IN POROUS MEDIA

Fluid flow in porous media plays an important role in a wide variety of technological and environmental processes such as chromatography, oil recovery, the degradation of building materials, and the spread of hazardous wastes in soils. The displacement of one fluid by another also exhibits a rich variety of pattern formation including a fractal or self-affine growth morphology. Such diverse behavior is a consequence of growth mechanisms that depend on the fluid properties (such as viscosity or surface tension), the structure of the porous media, and the external driving force that displaces the fluids. The complexity of single-component multiphase fluid flow in random porous media makes it theoretical and experimental study a great challenge.

The single component two-phase Lattice Boltzmann method was applied to the case of vapor displacement by liquid in a porous media. The simulations are carried out on a  $230 \times 100$  lattice, and the void space of the medium is represented as a collection of large pore bodies, called chambers, interconnected through narrow capillaries called throats. Such a representation has been repeatedly proved satisfactory for a variety of practical materials used in many fields. The pore network is initially filled with vapor and a fluid layer is set on the first several lattices. The internal walls use a simple bounce back boundary condition. Periodic boundaries are applied in the x direction and quasi-periodic boundary conditions were maintained in the y-direction.

Two cases were studied. In the first case we consider the invasion without wettability in the system. Fig.10 shows six snapshots of the simulation results. In

the second case, wettability is introduced to the system and leads to drastic changes in the displacement process. The desired wettability conditions can be implemented by assigning the surface adhesion parameter  $G_{ads}$  standing for the attractive force between fluid and solid. In this fashion, we take  $G_{ads} = -120$ , namely, the contact angle  $\theta = 0$  (completely wet). Fig.11 shows six snapshots of an imbibition simulation, where the liquid phase is assumed to wet the pore surface strongly, forming a thin liquid film along the pore walls. Compared with the case 1, breakthrough is attained more easily in this experiment, especially for the narrower throat. The liquid phase advances through the pore network through, mainly, film flow resulting in poor sweeping efficiency. It seems that the sweep form can overcome the capillary resistance. The gradual increases of the film thickness causes, eventually, snap-off at pore throats and entrapment of a large vapor quantity in pore chambers [10]. Continued application of an external gravity force causes, eventually, condensation of the trapped vapor, progressively from up to down and from smaller to larger pore chambers.

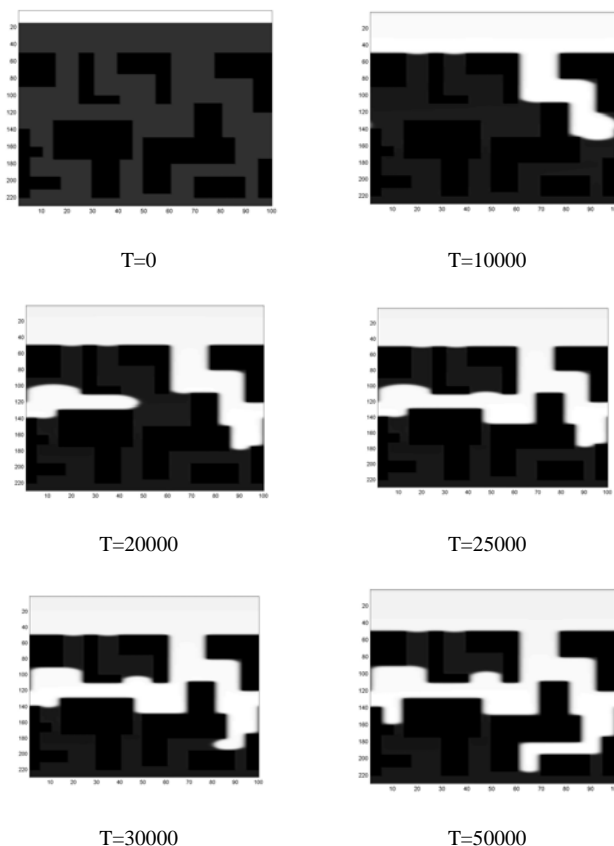


Fig.10 Displacement of vapor by liquid in porous media without wettability.

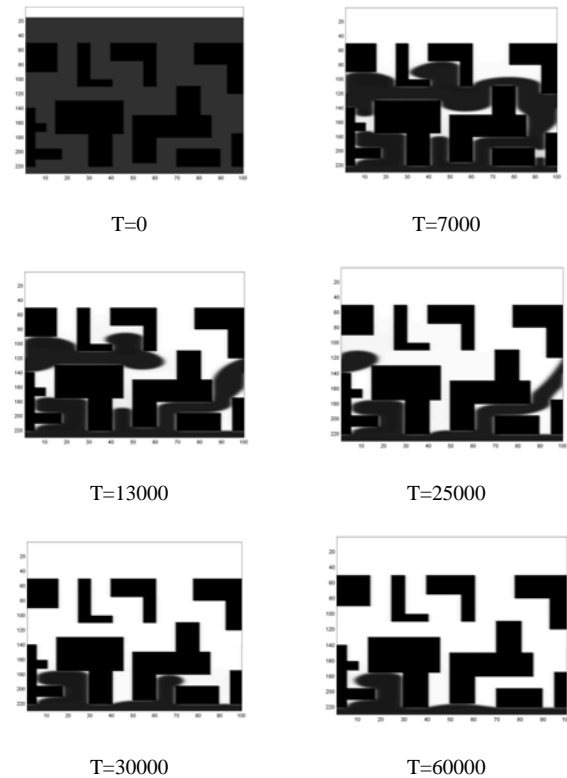


Fig.11 Displacement of vapor by liquid in porous media with strong wettability.

## V. CONCLUSION

To summarize, we have demonstrated the ability of single component multiphase LBM to simulate simultaneous liquid and vapor flow including contact angle and pipe flow. And the lattice-Boltzmann simulator was applied to two-phase flow problems in simple geometries and in pore networks. It was found that the simulator can predict several two-phase flow phenomena of critical significance in displacement applications, such as formation of advancing wetting film and early breakthrough under strong wettability conditions, film growth and snap off in throats, vapor condensation in pore, and wettability dependent sweeping efficiency of waterfloods. Furthermore, LBM provides insights into unstable and intermittent flows and interface routing in partially saturated pore networks that cannot be treated by standard continuum approaches such as the Richards equation

## ACKNOWLEDGMENT

The work was supported by the National Science Foundation of China, under Grant No. 41004052 and Project (HIT.NSRIF.2009135) supported by Natural Scientific Research innovation Foundation in Harbin Institute of Technology

## REFERENCE

- [1] Chen, S.; Chen, H.; Martinez, D. and Matthaeus, W., 1991, Lattice Boltzmann model for simulation of magnetohydrodynamics, *Phys. Rev. Lett.*, **67**(27), 3776.
- [2] Qian, Y. H.; d' Humières, D. and Lallemand, P., 1992, Lattice BGK models for Navier-Stokes equation, *Europhys. Letters*, **17**(6), 479.
- [3] Gunstensen, A. K.; Rothman, D. H.; Zaleski, S. and Zanetti, G., 1991, Lattice Boltzmann model of immiscible fluids, *Phys. Rev. A*, **43**(8), 4320.
- [4] Shan, X. and Chen, H., 1993, Lattice Boltzmann model for simulating flows with multiple phases and components, *Phys. Rev. E*, **47**(3), 1815.
- [5] Swift, M. R.; Osborn, W. R. and Yeomans, J. M., 1995, Lattice Boltzmann simulation of nonideal fluids, *Phys. Rev. Lett.*, **75**, 830.
- [6] He, X.; Shan, X. and Doolen, Gary D., 1998, Discrete Boltzmann equation model for nonideal gases, *Phys. Rev. E*, **57**(1), R13
- [7] Qian, Y. H.; d' Humières, D. and Lallemand, P., 1992, Lattice BGK models for Navier-Stokes equation, *Europhys. Letters*, **17**(6), 479.
- [8] Shan X. and Doolen G., 1995, Multicomponent lattice-Boltzmann model with interparticle interaction, *J. Stat. Phys.*, **81**, 379.
- [9] Dullien, F.A.L. Porous media: Fluid Transport and Pore Structure. Academic Press, San Diego, 1992, 554pp
- [10] O. Vizika, D. G. Avraam, and A. C. Payatakes. On the role of the viscosity ratio during low-capillary-number forced imbibition in porous media. *Journal of Colloid and Interface Science*. 1994, Vol.165, pp: 386-401